European Journal of Medicinal Chemistry 44 (2009) 1437–1451

Contents lists available at ScienceDirect

European Journal of Medicinal Chemistry

journal homepage: http://www.elsevier.com/locate/ejmech

Original article

Studies on self-aggregation of anthracycline drugs by restrained molecular dynamics approach using nuclear magnetic resonance spectroscopy supported by absorption, fluorescence, diffusion ordered spectroscopy and mass spectrometry

Prashansa Agrawal [a], Sudhir Kumar Barthwal [b], Ritu Barthwal [a,*]

[a] Department of Biotechnology, Indian Institute of Technology Roorkee, Roorkee 247667, India
[b] Department of Physics, Indian Institute of Technology Roorkee, Roorkee 247667, India

ARTICLE INFO

Article history:
Received 3 December 2007
Received in revised form
16 September 2008
Accepted 18 September 2008
Available online 7 October 2008

Keywords:
4′-Epiadriamycin, adriamycin and daunomycin
2D nuclear Overhauser enhancement spectroscopy
Restrained molecular dynamics
Electron spray ionization mass spectrometry
Diffusion ordered spectroscopy
Cardiotoxicity

ABSTRACT

Self-association, a process that competes with binding to DNA and formation of hetero-complexes, is studied in anticancer drugs 4′-epiadriamycin, adriamycin and daunomycin by proton nuclear magnetic resonance spectroscopy. The 2D nuclear Overhauser enhancement spectra yield several intra-molecular and inter-molecular inter-proton connectivities suggesting specific stacking patterns of aromatic chromophores in parallel and anti-parallel orientation. Absorption, emission and diffusion ordered spectroscopy demonstrate the formation of self-aggregates. Electron spray ionization mass spectrometry gives a direct proof of the presence of dimer and absence of higher aggregates. The restrained molecular dynamics simulations show the structural differences between drugs, which have been correlated to the biological action. A clear evidence of reduced cardiotoxicity by 4′-epiadriamycin, as compared to daunomycin and adriamycin, is demonstrated by mass spectrometry data.

1. Introduction

Anthracycline antibiotics are highly active anticancer compounds that have found considerable clinical use [1]. They bind to both DNA and the DNA binding protein topoisomerase-II. The biological activities of different anthracycline based drugs depend on the minor modifications in their chemical structure [2]. Among them, daunomycin, adriamycin (in which one hydrogen atom of methyl group of 9$COCH_3$ moiety at carbon 14 position of daunomycin is replaced by a hydroxyl group that is, 9$COCH_2OH$), 4′-epiadriamycin, (epimer of adriamycin, differs at the 4′-position of the daunosamine sugar) are worth mentioning (Fig. 1). The 4′-epiadriamycin, developed recently is better tolerated due to lesser cardiotoxicity in comparison to daunomycin and adriamycin [3]. These drugs are isolated from cultures of *Streptomyces caeruleorubidus* with cytotoxic and anti-mitotic activity. They are localized in the nucleus. They are believed to exert their biological activity by intercalating into the DNA double helix and act by inhibition of both DNA replication and RNA transcription.

In aqueous solution, anthracycline drugs are reported to self-associate [4–9]. Several studies on concentration-dependent absorbance [7], proton NMR [5] and circular dichroism [5,8] spectra have been interpreted in terms of simple dimerization model. These drugs are known to aggregate beyond the dimer insignificantly in most cases, although Barthalemy-Clavey et al. [5] did suggest that further aggregation might occur at drug concentrations $\geq$5 mM. Prior to determination of the structural and thermodynamical characteristics of intercalative binding of aromatic drugs to known DNA sequences by NMR spectroscopy [10–13], it is necessary to determine the self-association of drugs in solution. The drugs are known to form hetero-association complexes with polyphenols, xanthines, flavanoids, etc., consumed as a part of food intake [14]. Both self-associated as well as hetero-complexes affect their transport across bilayer lipid membrane [14,15]. These factors influence the anticancer action and hence are clinically important.

Our primary focus is to investigate the precise manner in which the anthracycline drugs self-aggregate in solution and correlate

* Corresponding author. Tel.: +91 1332 285807/484; fax: +91 1332 273560.
E-mail addresses: ritubfbs@iitr.ernet.in, ritubarthwal@yahoo.co.in (R. Barthwal).

0223-5234/$ – see front matter © 2008 Elsevier Masson SAS. All rights reserved.
doi:10.1016/j.ejmech.2008.09.037

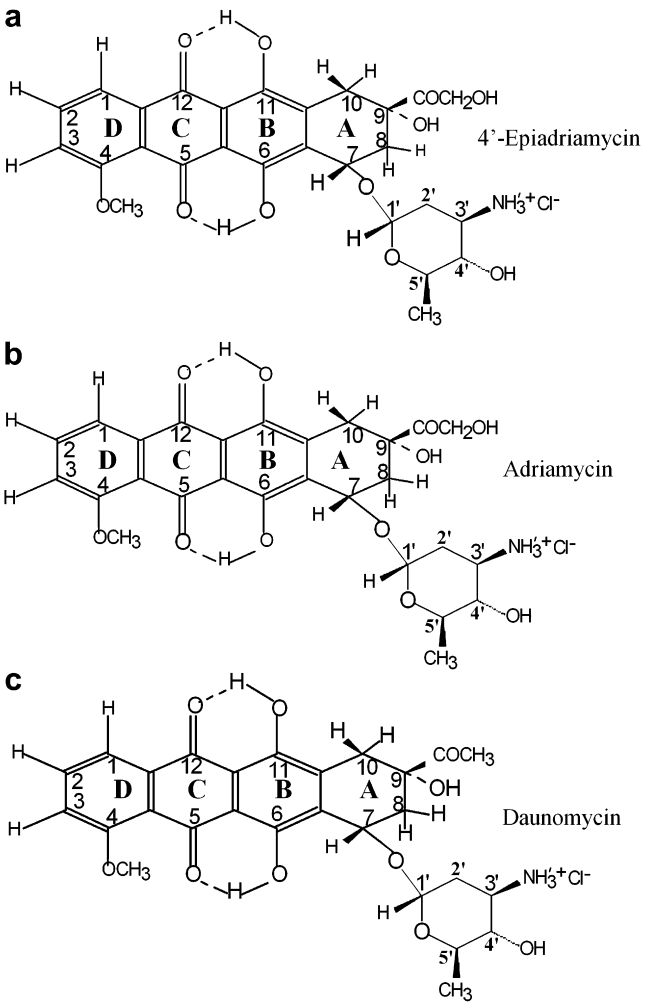

Fig. 1. Chemical structure of (a) 4′-epiadriamycin, (b) adriamycin and (c) daunomycin.

them to their biological activity. We have carried out the proton NMR investigations on 4′-epiadriamycin, adriamycin and daunomycin in solution using 1D and 2D NMR techniques as a function of concentration and temperature. A molecular model is built using restraints obtained from the Nuclear Overhauser Enhancement (NOE) data to get preferred conformations of the dimer. To date no such restrained Molecular Dynamics (rMD) simulations have been reported for 4′-epiadriamycin.

The Diffusion Ordered Spectroscopy (DOSY) [16] distinguishes between complexed, uncomplexed and self-aggregated forms in a mixture due to the differences in their relative values of translational diffusion coefficient. A change in chemical shift does not provide sufficient indication about the strength of interaction between the components, which could be due to other effects influencing the chemical structure. On the other hand DOSY plots clearly manifest strength of hydrogen bonding [17]/ligand binding [18] and self-association [19] which may help in structure elucidation. Also, spins in two different chemical surroundings may be identified separately depending upon their diffusion coefficient, diffusion time and relative populations of spins [20]. Absorption and fluorescence studies have also been carried out as a function of concentration to ascertain independently the self-aggregation of drugs. Electron Spray Ionization Mass Spectrometry (ESI-MS) [21,22] has since been introduced as a sensitive and specific tool for the analysis of specific non-covalent complexes. It probes purely inter-molecular interactions in the absence of solvent, preserving even very weak interactions during the transfer of ions from the liquid to gas phase. A significant advantage of ESI over other soft ionization techniques is that samples can be analyzed directly in aqueous solutions under conditions very similar to those occurring in biological fluids, without alien additions. It has been successfully employed for the analysis of specific associations involving dimer and higher aggregates of nucleic acids [23]. We have used DOSY and ESI-MS for the first time to provide the direct proof of self-association of these drugs. The structural differences between the rMD structures based on NMR data have been correlated to the results obtained from other physico-chemical techniques and biological activity.

2. Results and discussion

2.1. NMR studies

Fig. 2a–c shows the proton NMR spectra of 4′-epiadriamycin, adriamycin and daunomycin at some of the concentrations at 298 K in D_2O. The variation in chemical shifts is given in supplementary information, SI 1–3. An increase in concentration from 0.01 to 8.00 mM leads to upfield shift in the aromatic ring D protons, 1H, 2H, 3H, $4OCH_3$ up to $\Delta\delta = 0.52$ ppm (Table 1a). The ring A protons 10axH, 10eqH, 8axH, 8eqH, also show significant upfield shifts up to 0.68 ppm. These are in accord with earlier observations on daunomycin reported in literature [4,15,24,25] and have been attributed to stacking of aromatic rings forming self-aggregates. No such studies have been carried out so far for adriamycin and 4′-epiadriamycin to the best of our knowledge. The 4′-epiadriamycin and adriamycin differ in their structure only by an inversion of the substituents H and OH at C4′ position of the sugar moiety. We observe that there are substantial differences in $\Delta\delta$ values (0.21–0.46 ppm) of ring A protons, 8eqH, 10axH, 10eqH, 7H due to stacking. The difference is evident (0.09–0.16 ppm) in 3′H, 4′H, 5′H and $4OCH_3$ protons as well. This indicates that the self-associated structures in 4′-epiadriamycin are different from that of adriamycin.

We have also examined the NMR spectra of drugs alone at 8 mM concentration as a function of temperature (Fig. 3a–c). We observe considerable differences among the three drugs (Table 1b). The ring D protons 1H, 2H, 3H, reflect large downfield shifts up to 0.81 ppm with temperature which may be due to de-stacking in self-aggregated structures. However, there are other factors such as change in (i) monomer–dimer equilibrium (ii) hydrogen bonding if present and (iii) structural changes, which contribute towards change in chemical shift with temperature. It is noteworthy that there are significant differences in $\Delta\delta_{355-275\ K}$ of 7H, 10eqH, 3′H, 1H, 2H and 3H protons in 4′-epiadriamycin and adriamycin. The 4′OH, 9OH, 6OH and 11OH are observed in NMR spectra of 4′-epiadriamycin but not in that of adriamycin and daunomycin. Apparently these protons are immobilized in stacked/self-aggregated structure of 4′-epiadriamycin. They are free and may be exchanging with solvent rapidly in daunomycin and adriamycin and therefore are not observable in their NMR spectra. These observations clearly are indicative of the fact that stacked structure in 4′-epiadriamycin is different from those of both, adriamycin and daunomycin.

Analysis of 2D NOESY spectra at 355 K (Figs. 4a,b, 5a,b and 6a,b) shows the presence of several inter-proton contacts (Table 2), for which the distances have been calculated. The corresponding distances in the rMD simulated structures are close to experimental restraints (Table 2) and hence are true representative of the experimental results. Several NOE connectivities, e.g. 5′CH_3–1′H, 8eqH–10axH, 8eqH–1′H, etc. (SI 4) show proximity of protons within daunosamine sugar, within ring A, within ring D as well as proximity of ring A protons to daunosamine sugar [24]. These intramolecular connectivities characterize specific conformation of ring A and daunosamine sugar in each drug. Several NOE contacts such as

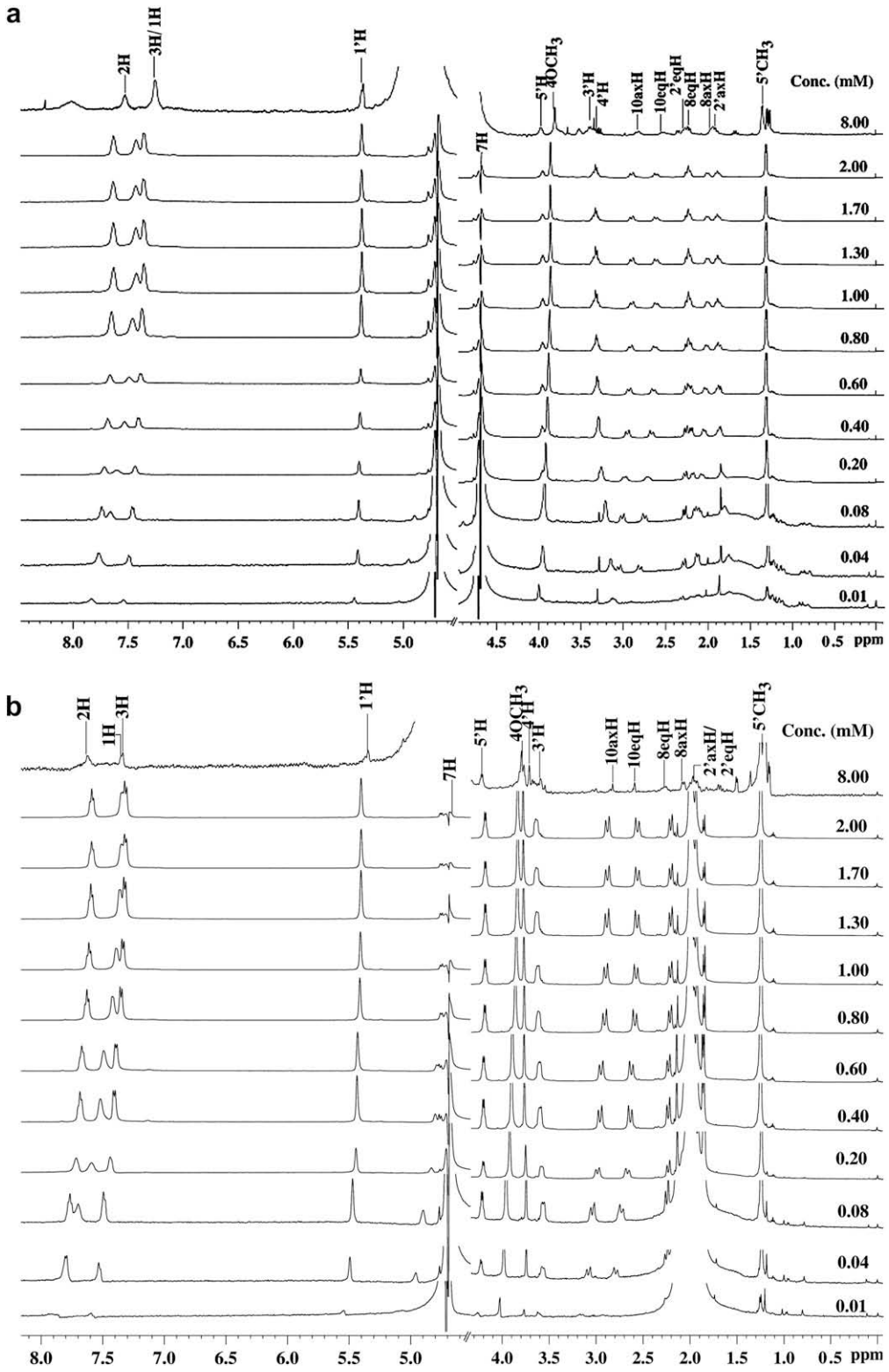

Fig. 2. (a) 1D proton NMR spectra of 4′-epiadriamycin in D_2O as a function of concentration (0.01–8.00 mM) at 298 K. (b) 1D proton NMR spectra of adriamycin in D_2O as a function of concentration (0.01–8.00 mM) at 298 K. (c) 1D proton NMR spectra of daunomycin in D_2O as a function of concentration (0.01–8.00 mM) at 298 K.

2H–10eqH/10axH/9COCH$_2$/7H/8axH/5′CH$_3$; 4OCH$_3$–10axH/10eqH/8axH/8eqH/9COCH$_2$/7H; 1H/3H–8axH/10axH/10eqH/9COCH$_2$/7H in adriamycin are possible only if aromatic chromophores of two drug molecules overlap in a stacked structure forming dimer in which ring A lies above ring D, hence in an anti-parallel orientation (Table 2). Several other NOE connectivities, e.g. 5′CH$_3$–10axH/10eqH, 1′H–10eqH/9COCH$_2$, 3′H–9COCH$_2$/10axH also refer to inter-molecular contacts but in parallel orientation of aromatic chromophores in which ring A is stacked over ring A itself. Evidence of such dimer structures in parallel and antiparalel orientations were found for the first time by Evstigneev et al. [15] in daunomycin molecule at 303 K. However, since 7H–10axH/10eqH cross-peak is observed in parallel

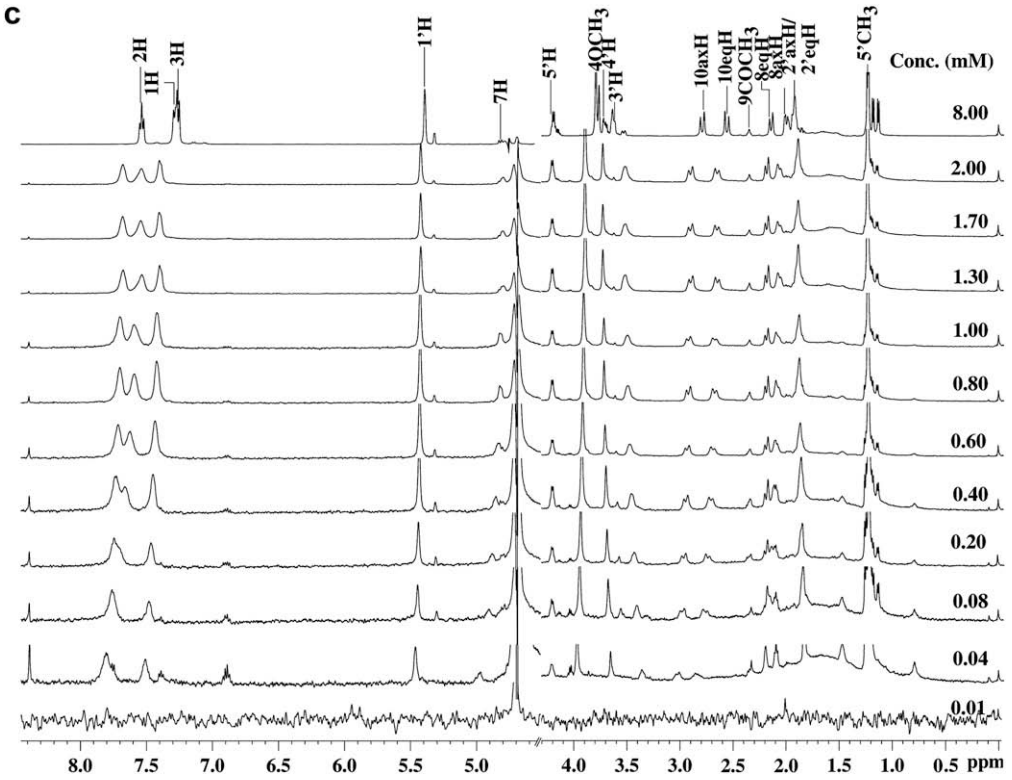

Fig. 2. (*continued*).

mode of orientation, the ring A is stacked over ring A but is inverted. This is also evident from the orientation of $4OCH_3$ moiety, which is lying in opposite sense in the two stacked molecules in the structure obtained after rMD simulations (Fig. 7a–c). The parallel mode of orientation is therefore different from that of Evstigneev et al. [15]. Our results show more cross-peaks than that observed by Evstigneev et al. [15]. These are: (a) in parallel orientation, 7H–10axH/10eqH; 10axH/10eqH–1′H/2′eqH/2′axH/4′H; $9COCH_2$/$9COCH_3$–1′H/2′eqH/2′axH/3′H/4′H/5′H/7H and (b) in anti-parallel orientation, $9COCH_2$/$9COCH_3$–1H/$4OCH_3$; 7H–$4OCH_3$; 1′H–$4OCH_3$; 2′eqH/2′axH–1H/2H/3H/$4OCH_3$; 3′H–1H/2H/$4OCH_3$; 4′H–1H/2H/3H/$4OCH_3$; 5′CH_3–$4OCH_3$.

We also observe differences among the three drugs. For example, it is seen that in anti-parallel orientation, $9COCH_3$–2H/3H cross-peak is absent in daunomycin but is present in adriamycin and 4′-epiadriamycin ($9COCH_2$–2H/3H). This may be due to hydrophilicity of $9COCH_2$ group, which permits ordering of water molecule around it as compared to $9COCH_3$ group. The cross-peaks 4′H–1H, 10axH–3′H/4′H; 10eqH–4′H present in adriamycin and daunomycin are absent in 4′-epiadriamycin, which may be attributed to inversion of the H and OH at 4′ position of adriamycin/daunomycin sugar moiety. Thus, our results show that self-association observed by Evstigneev et al. [15] in daunomycin exists in its analogues, adriamycin and 4′-epiadriamycin as well. The self-associated structures

Table 1a
Changes in chemical shift $\Delta\delta$ (in ppm) of drug protons due to change in concentration of drugs, 4′-epiadriamycin (EPIADM), adriamycin (ADM) and daunomycin (DNM) in D_2O solvent and its comparison with literature.

	$\Delta\delta$ ($\delta_{8.00} - \delta_{0.01\ mM}$)			$\Delta\delta$ ($\delta_{3.5} - \delta_{0.1\ mM}$)	$\Delta\delta$ ($\delta_{7.0} - \delta_{0.5\ mM}$)	$\Delta\delta$ ($\delta_{7.0} - \delta_{0.5\ mM}$)
	298 K (present work)			303 K [15]	298 K [4]	323 K [4]
	EPIADM	ADM	DNM	DNM	EPIADM	ADM
5′CH_3	+0.01	+0.02	−0.05	–	–	–
2′axH	+0.04	−0.01	+0.05	–	–	–
8axH	−0.18	−0.24	−0.26	–	–	–
8eqH	+0.04	−0.28	−0.27	0.05	–	–
2′eqH	−0.05	−0.01	+0.05	–	–	–
10axH	−0.40	−0.68	−0.38	0.16	–	–
10eqH	−0.28	−0.49	−0.30	0.19	–	–
4′H	+0.20	+0.04	+0.08	–	–	–
3′H	+0.19	+0.10	+0.21	–	–	–
$4OCH_3$	−0.16	−0.30	−0.24	0.17	−0.32	−0.22
5′H	−0.04	−0.17	+0.02	–	–	–
7H	+0.37	+0.01	−0.36	–	0.00	0.00
$9COCH_3$	–	–	+0.02	0.01	–	–
1′H	−0.11	−0.12	−0.16	0.08	–	–
3H	−0.31	−0.28	−0.34	0.24	−0.26	−0.23
1H	−0.57	−0.52	−0.54	0.43	−0.38	−0.37
2H	−0.33	−0.37	−0.34	0.25	−0.21	−0.20

Downfield shift is +ve; upfield shift is −ve.

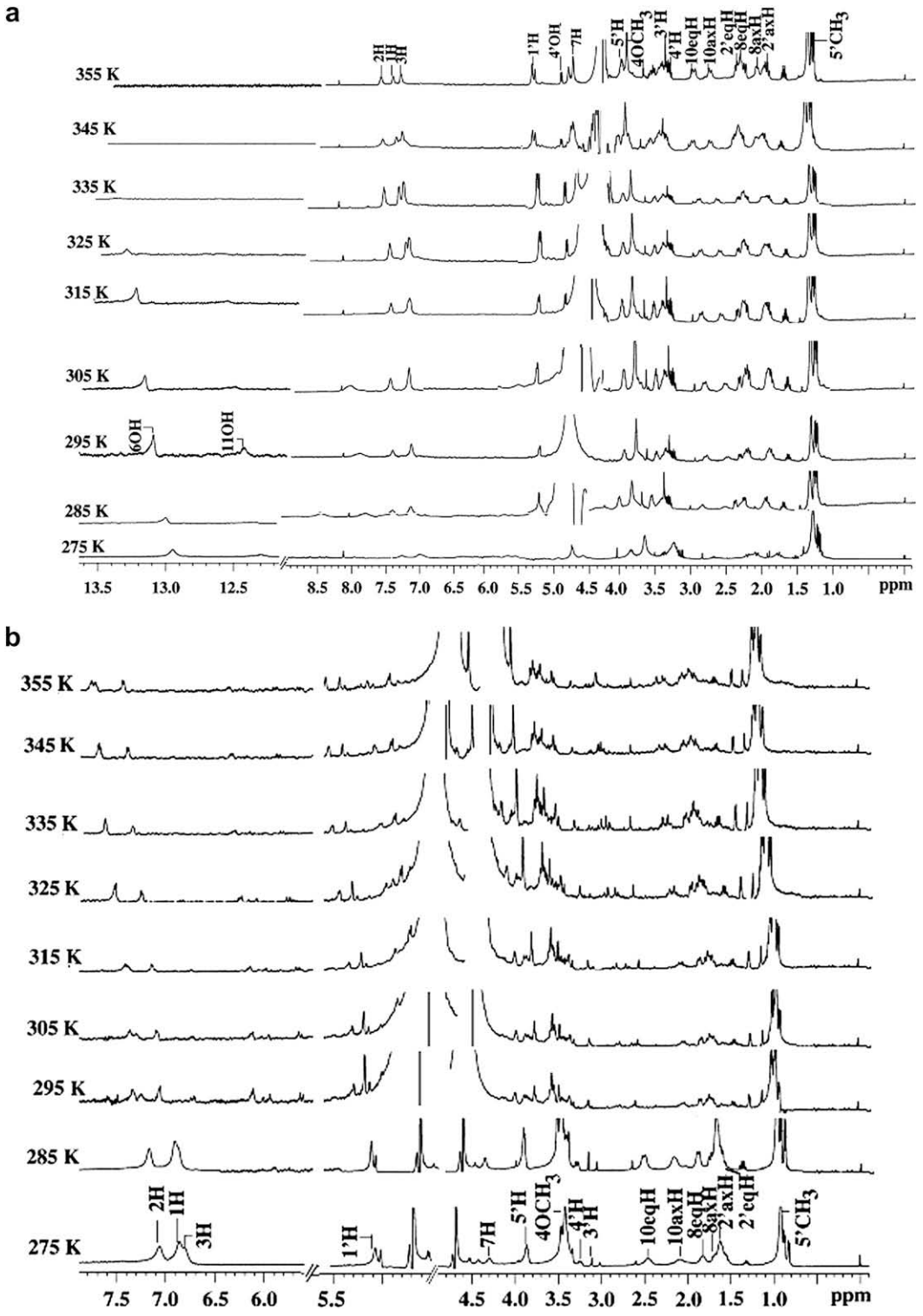

Fig. 3. (a) 1D proton NMR spectra of 8 mM 4′-epiadriamycin in D_2O as a function of temperature (275–355 K). (b) 1D proton NMR spectra of 8 mM adriamycin in D_2O as a function of temperature (275–355 K). (c) 1D proton NMR spectra of 8 mM daunomycin in D_2O as a function of temperature (275–355 K).

are, however, specific in each case owing to difference in the chemical groups.

2.2. Restrained Molecular Dynamics (rMD) studies

The dimer models of the drugs are build by using short, medium and long inter-proton distances (Table 2 and SI 4) categorized as NOEs having strong, medium, and weak intensity with the corresponding distances set in the range 1.8–2.4 Å, 2.5–2.9 Å, and 3.0–4.5 Å, respectively. The models of the drugs obtained from rMD simulations (Fig. 7a–c) show that there is significant overlap of the aromatic rings and the daunosamine amino sugar. Upfield shift in 2H, 3H and 1H protons upto 0.56 ppm may be due to magnetic shielding arising from ring currents of π electrons. The daunosamine sugar moiety of one molecule of the drug interacts with the chromophore of the other molecule of the same drug and vice

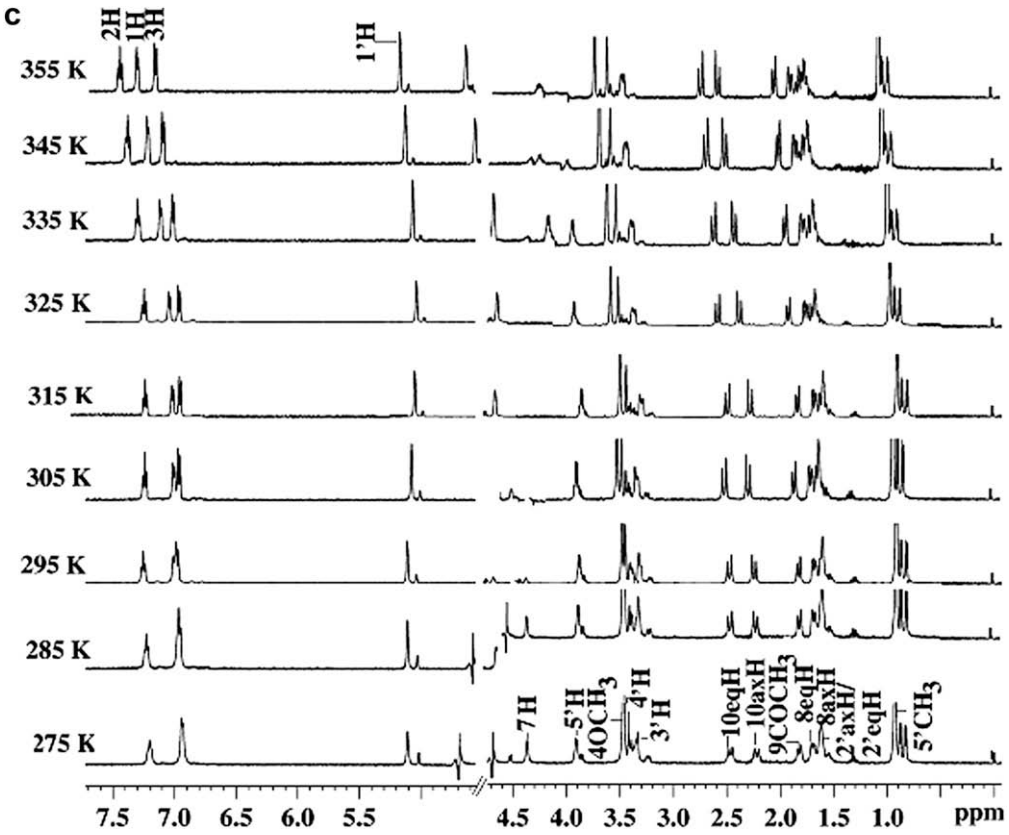

Fig. 3. (*continued*).

versa, thus there is possibility of H-bond formation between the O12 atoms of aromatic ring C of the chromophore of one molecule and the NH_3^+ group of the amino sugar ring of the other in daunomycin. This bond is absent in 4′-epiadriamycin and adriamycin. Adriamycin and 4′-epiadriamycin show 6O–H···O5′ hydrogen bond, having a distance of 2.79 Å. Besides this, few van der Waals interactions are also present: 5′CH_3–6O (2.19 Å) in parallel orientation of 4′-epiadriamycin and 12C–6O (2.50 Å) in anti-parallel orientation of adriamycin. The total energy obtained after rMD simulations is 181, 177 and 151 kcal/mol for daunomycin, adriamycin and 4′-epiadriamycin, respectively in the anti-parallel orientation. On the other hand, the corresponding energy for parallel orientation is 325, 297 and 294 kcal/mol, respectively. The mole fraction of conformer with parallel orientation is small compared to that of conformer with anti-parallel orientation due to higher total energy. The aggregation of aromatic molecules is known to be driven by stacking interactions, in which the main components are dispersive and van der Waals attractions. The angle between planes of aromatic rings of two molecules of dimer in 4′-epiadriamycin is lower (13° for parallel and 38° for

Table 1b
Change in chemical shift per unit change in temperature, $\Delta\delta/\Delta T$ (in ppb/K) of 4′-epiadriamycin (EPIADM), adriamycin (ADM) and daunomycin (DNM) protons in D_2O and its comparison with literature.

	$(\delta_{355}-\delta_{275\ K})/\Delta T$			$(\delta_{335}-\delta_{278\ K})/\Delta T$	$(\delta_{348}-\delta_{283\ K})/\Delta T$	$(\delta_{355}-\delta_{277\ K})/\Delta T$	$(\delta_{355}-\delta_{277\ K})/\Delta T$	$(\delta_{350}-\delta_{277\ K})/\Delta T$
	8.0 mM (present work)			1.6 mM [15]	7.0 mM [4]	11.5 mM [24]	11.5 mM [24]	4.95 mM [25]
	EPIADM	ADM	DNM	DNM	DNM	ADM		EPIADM
5′CH_3	0.3	1.0	1.4	–	–	2.4	2.3	−0.1
2′axH	1.5	2.0	1.6	–	–	2.6	1.9	0.1
8axH	2.9	1.4	1.8	–	–	3.3	3.5	1.1
8eqH	1.0	0.4	2.1	–	–	3.7	3.5	1.2
2′eqH	0.4	2.0	1.6	–	–	2.6	1.9	0.5
10axH	3.5	0.3	4.1	–	–	5.8	5.9	2.2
10eqH	2.6	−1.5	2.9	2.3	–	4.0	4.2	1.6
4′H	1.0	3.1	2.1	–	–	2.7	2.2	−0.1
3′H	1.0	0.6	1.0	–	–	2.1	1.7	−1.0
4OCH_3	2.1	2.0	2.8	–	2.8	3.6	4.1	1.5
5′H	0.7	1.3	0.9	−0.4	–	2.1	1.8	−0.4
7H	−1.4	7.3	3.6	–	–	1.9	5.3	1.9
9$COCH_3$	–	–	2.4	–	0.0	5.3	–	0.0
1′H	−0.3	2.9	1.0	–	–	2.2	2.1	−0.3
3H	2.4	7.3	3.1	–	5.1	3.8	4.4	2.3
1H	3.3	10.1	4.6	–	4.0	5.6	6.7	2.7
2H	2.5	7.5	3.4	3.0	3.1	4.4	4.9	2.1

Downfield shift is +ve; upfield shift is −ve.

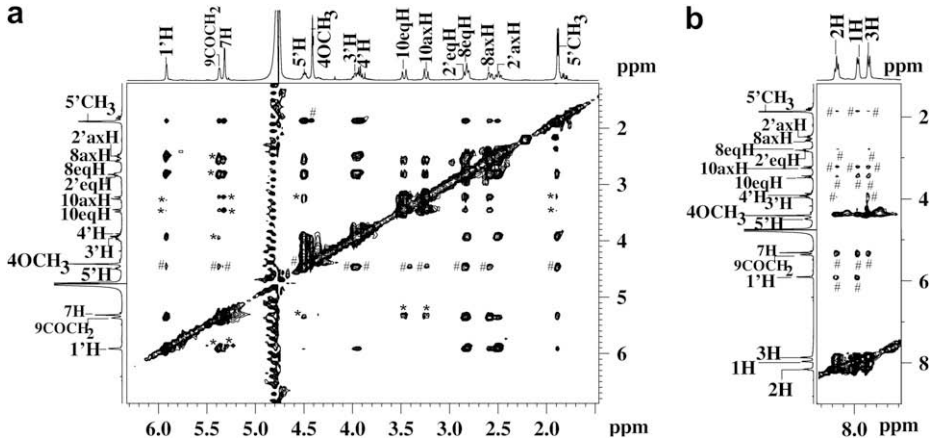

Fig. 4. (a–b) 2D NOESY spectra of 8 mM 4′-epiadriamycin in D_2O at 355 K at 500 MHz. The figure shows expansions of specific regions to highlight connectivities. (* Indicates parallel and # anti-parallel mode of orientation.)

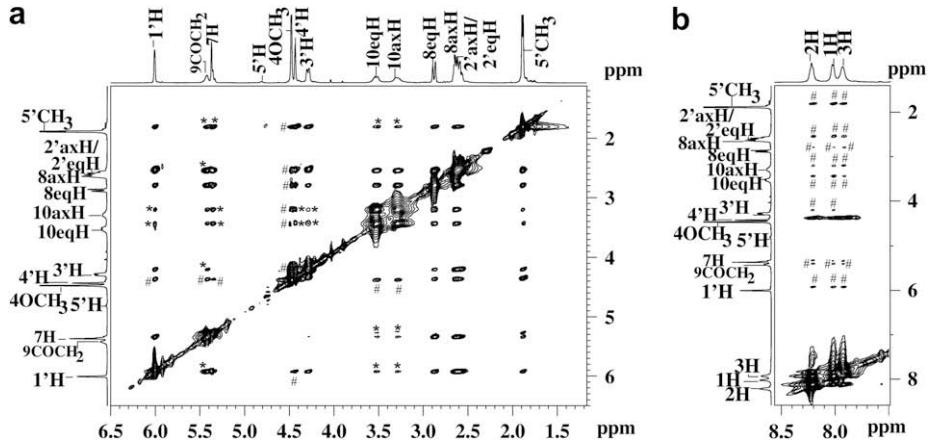

Fig. 5. (a–b) 2D NOESY spectra of 8 mM adriamycin in D_2O at 355 K at 500 MHz. The figure shows expansions of specific regions to highlight connectivities. (# Indicates anti-parallel orientation and * parallel mode of orientation.)

anti-parallel mode) in comparison to that of adriamycin (40° for parallel and 78° for anti-parallel mode) and daunomycin (62° for parallel and 83° for anti-parallel mode) indicating that 4′-epiadriamycin is better stacked. It is noteworthy that glycosidic torsional angle C7–O7–C1′–C2′ in 4′-epiadriamycin, adriamycin and daunomycin is −149° (parallel), −143° (anti-parallel); −157° (parallel), −135° (anti-parallel) and −169° (parallel), −148° (anti-parallel), respectively. This angle is involved in anchoring of drug chromophore and positioning of daunosamine sugar between base pairs of DNA in the drug–DNA complex. It has been shown [26] that

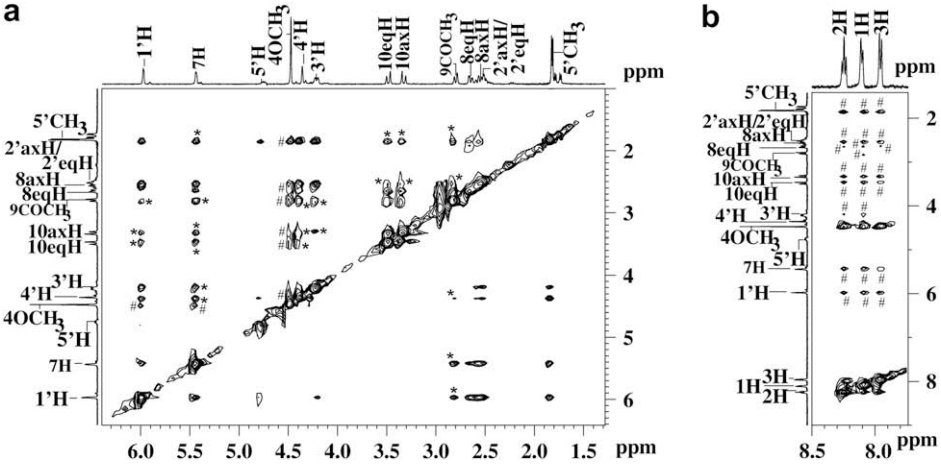

Fig. 6. (a–b) 2D NOESY spectra of 8 mM daunomycin in D_2O at 355 K at 500 MHz. The figure shows expansions of specific regions to highlight connectivities. (# Indicates anti-parallel orientation and * parallel mode of orientation.)

Table 2
Connectivities and inter-proton distances (Å) of 4′-epiadriamycin, adriamycin and daunomycin obtained from NOESY spectra ($\tau_m = 400$ ms) at 355 K. The corresponding distances obtained from optimized rMD structure are also shown. 's' is short (1.8–2.4 Å), 'm' is medium (2.5–2.9 Å) and 'l' is long (3.0–4.5 Å) inter-proton distance. Distances greater than 4.5 Å is denoted by 'ww'. Overlap of peak is shown by 'o' and '–' indicates absence of peak. '**E**' denotes NOE observed for daunomycin at 303 K by Evstigneev et al. [15].

Connectivities	4′-Epiadriamycin (Å)		Adriamycin (Å)		Daunomycin (Å)	
	NMR	rMD	NMR	rMD	NMR	rMD
Parallel orientation connectivities						
7H–10axH	l	3.67	l	3.44	l	3.20
7H–10eqH	l	4.46	l	3.48	l	3.31
10axH–1′H	ww	–	ww	4.59	l	4.78
10axH–4′H	–	–	o	–	s	2.12
10axH–3′H, **E**	–	–	l	4.17	l	3.34
10axH–5′H, **E**	ww	4.33	–	–	–	–
10axH–5′CH_3, **E**	ww	4.79	ww	4.76	l	4.41
10eqH–1′H	ww	4.81	l	3.96	l	3.91
10eqH–3′H, **E**	–	–	l	4.15	–	–
10eqH–4′H	–	–	o	–	s	2.20
10eqH–5′H, **E**	–	–	–	–	–	–
10eqH–5′CH_3, **E**	l	4.68	l	3.73	l	3.90
9$COCH_2$/9$COCH_3$–3′H	–	–	ww	4.59	ww	4.37
9$COCH_2$/9$COCH_3$–5′H	l	4.63	–	–	–	–
Anti-parallel orientation connectivities						
10axH–1H, **E**	ww	4.80	l	4.32	ww	4.59
10axH–2H, **E**	l	4.56	l	4.17	l	4.39
10axH–3H, **E**	l	4.31	l	3.64	l	3.48
10axH–4OCH_3, **E**	l	4.65	ww	4.70	l	3.12
10eqH–1H, **E**	l	4.39	ww	4.72	l	4.42
10eqH–2H, **E**	l	4.07	l	3.92	l	4.14
10eqH–3H, **E**	l	3.78	m	2.54	l	4.33
10eqH–4OCH_3, **E**	l	4.45	l	4.72	l	3.18
9$COCH_2$/9$COCH_3$–2H	o	–	l	4.45	–	–
9$COCH_2$/9$COCH_3$–3H	o	–	l	4.31	–	–
8eqH–1H, **E**	l	3.02	l	4.16	l	3.88
8eqH–2H, **E**	–	–	l	4.20	l	3.94
8eqH–3H, **E**	l	3.55	l	4.45	l	4.16
8eqH–4OCH_3, **E**	o	–	ww	4.67	o	–
8axH–1H, **E**	–	–	o	–	l	3.94
8axH–2H, **E**	–	–	o	–	l	3.06
8axH–3H, **E**	–	–	o	–	l	3.88
8axH–4OCH_3, **E**	o	–	m	2.67	o	–
7H–1H, **E**	o	–	l	4.43	m	2.58
7H–2H, **E**	o	–	l	4.06	l	3.27
7H–3H, **E**	o	–	l	4.61	l	3.42
1′H–1H, **E**	l	3.46	m	2.96	l	3.07
1′H–2H, **E**	l	3.20	l	3.74	l	4.02
1′H–3H, **E**	–	–	m	2.49	l	3.27
2′eqH/2′axH–1H	–	–	o	–	o	–
2′eqH/2′axH–4OCH_3	o	–	–	–	o	–
3′H–1H	–	–	l	4.81	l	4.02
3′H–2H	–	–	l	3.76	ww	5.03
4′H–1H	–	–	o	–	o	–
5′CH_3–1H, **E**	ww	4.80	ww	4.72	l	3.91
5′CH_3–2H, **E**	ww	4.87	l	4.17	l	4.38
5′CH_3–3H, **E**	ww	4.99	ww	4.19	l	4.02
5′H–4OCH_3	o	–	–	–	ww	–

this angle can adopt three conformations, that is, (1) 156–167° (2) 127–144° (3) 38–78°. Our rMD structure shows that 4′-epiadriamycin adopts only (2) conformer in both parallel and anti-parallel orientations while adriamycin and daunomycin adopt conformation (1) in parallel mode and conformation (2) in anti-parallel mode of orientation. This feature has important implications in biological action of these drugs, and is discussed later.

2.3. Absorption and emission studies

The absorption spectra of drugs show three bands in the visible region (529, 496, 479 nm) and three in the ultraviolet range (288, 252, 233 nm) [27]. The three visible region bands are characteristic of the conjugated anthracycline rings; in the ultraviolet region, one at 288 nm is for aromatic ring and the other two, that is, 252, 233 nm are for daunosamine sugar moiety of the drugs. As the concentration of drug increases, there are weak but definite changes in the shape of their spectra. The maxima located at 288 and 496 nm vanish, while the absorption increases in the wavelength range 200–400 nm. For lower concentration (~6–7 μM), the absorption follows the Beer–Lambert law. For higher concentrations, deviations are observed. In dilute solution (1 μM) the 496 and 479 nm bands are of equal intensity, while in concentrated solution (12 μM), the spectrum is broader and the 496 nm band becomes less intense relative to the 479 nm band (Fig. 8). The chromophores of the anthracyclines are planar. There is uneven electronic charge distribution and such a charge distribution could favour the formation of stacked dimers. Using excitation wavelength (λ_{ex}) as 480 nm and emission wavelength (λ_{em}) as 592 nm, the emission scan was done in Spectrofluorimeter (make HORIBA Jobin, Horiba model Fluorolog-3). Fluorescence intensity gets quenched when the drugs start forming dimer. Since the dipole moment of the monomer–dimer transition is zero, observed fluorescence is mainly contributed by the monomer species (Fig. 9). Also, there is no shift in the emission maxima with increase in concentration. The dimerization constant (K_D) is calculated by computer-aided extrapolation of the spectral changes to high dilution of the drugs, that is, least square-fitting curve using software MATLAB 7.0 version. The concentration of monomer, dimer and the dimerization constant is calculated and the values are of the order of 10^5 M^{-1} for all the three drugs, which are close to that obtained by Chaires et al. [4]. It may be noted that there is a possibility of the existence of higher aggregates at higher concentration.

2.4. Diffusion Ordered Spectroscopy (DOSY) studies

The DOSY technique has been developed to facilitate the complex mixture analysis without physical separation. The drugs are known to exhibit self-association at the concentration used. Our results show that the rate of exchange between monomer and dimer is apparently fast; therefore instead of two peaks only one peak is observed, which is averaged value of each weighted by its relative concentration. Adriamycin shows a diffusion rate, which is intermediate between that of 4′-epiadriamycin and daunomycin, while daunomycin shows fastest diffusion (Fig. 10a–c). The diffusion coefficient is $1.84 \pm 0.09 \times 10^{-11}$ m^2/s for 4′-epiadriamycin, $2.89 \pm 0.11 \times 10^{-11}$ m^2/s for adriamycin and $1.52 \pm 0.19 \times 10^{-11}$ m^2/s for daunomycin at 275 K. At 298 K, the corresponding values increase in the same order being $1.53 \pm 0.19 \times 10^{-10}$ m^2/s, $1.63 \pm 0.21 \times 10^{-10}$ m^2/s and $2.10 \pm 0.29 \times 10^{-10}$ m^2/s, respectively (Fig. 10a–c). Since the rates are weighted by the relative concentrations of monomer and aggregated forms, it may be inferred that greater extent of self-aggregation exists in 4′-epiadriamycin.

2.5. Electron Spray Ionization Mass Spectrometry studies (ESI-MS)

The electron spray ionization mass spectrometric studies of the three anthracycline drugs (Fig. 11) show that the drugs exist in monomeric as well as dimeric state at 5 μM concentration in singly charged state. Adriamycin and 4′-epiadriamycin are epimers with same molecular weight; their intense peaks appear at 545 m/z ratio whereas for daunomycin it appears at 528 m/z ratio for the monomeric forms. Their dimeric species exist at 1089 and 1056 m/z, respectively, corresponding to the molecular weight of the dimers with single charge. We did not observe any peak corresponding to trimer or higher aggregates with single/double charge. The mass spectrum gives a direct proof of the existence of dimer species due to self-aggregation and absence of trimer or higher aggregates.

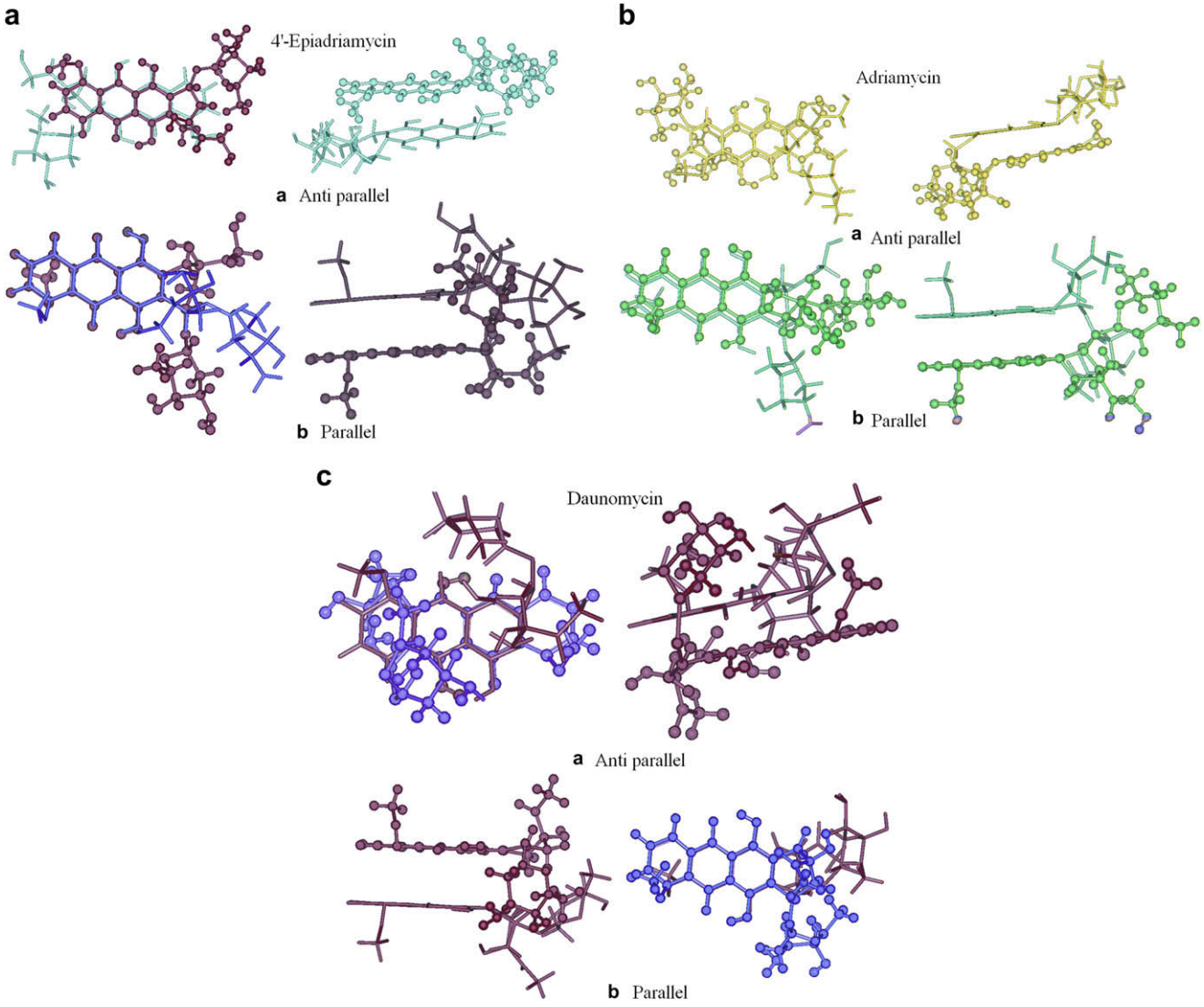

Fig. 7. (a) Structure of self-associated dimer of 4′-epiadriamycin based on restrained molecular dynamics simulations using experimental distance restraints from NOESY spectra. (b) Structure of self-associated dimer of adriamycin based on restrained molecular dynamics simulations using experimental distance restraints from NOESY spectra. (c) Structure of self-associated dimer of daunomycin based on restrained molecular dynamics simulations using experimental distance restraints from NOESY spectra.

However, it may be noted that Fig. 11 cannot be used to give a quantitative estimate of the relative amount of monomer and dimer since the process of electron spray ionization in gaseous phase may cleave the dimers or higher aggregates, if present. We observe a peak at $m/z = 908$ in mass spectra of daunomycin. This mass number corresponds to dimer ($m/z = 1056$) without daunosamine sugar moiety ($m/z = 148$). Similar peak is observed at $m/z = 941$ in adriamycin whereas no such corresponding signal is seen in 4′-epiadriamycin. This shows that cleavage is higher in daunomycin as compared to adriamycin while 4′-epiadriamycin does not show cleavage at all.

2.6. Biological relevance

2.6.1. Anticancer action

The anthracycline antibiotics are among the most effective antitumor medicines used in clinics for medicinal treatment of various types of malignant tumors. The dose of drugs is generally more than tens of micromolar concentration. Self-aggregation takes place at these high concentrations, which will compete with binding to target DNA. The thermo-dynamical and structural analysis of intercalative binding of these drugs to DNA sequence therefore requires a precise pre-knowledge of self-association. The self-aggregation of these drugs also plays a biological role in influencing the selective transport of these substances through cell membrane as well as multiple drug resistance caused by proteins forming channels in bilayer lipid membrane [14,15]. Besides, several naturally occurring aromatic molecules consumed as a part of food (e.g. methyl xanthines, polyphenols) associate with these drugs. Alternately these drugs are used in combination with some aromatic molecules [28,29]. It has been shown that caffeine (present in tea, coffee, coca, chocolate) forms hetero-association complexes with number of anticancer aromatic drugs, which effectively lowers the concentration of free ligands and thereby reduces the pharmacological activity of drugs. The major mechanism responsible for marked reduction in toxicity of adriamycin in cultured cell lines treated with caffeine [30,31] was found to be formation of adriamycin–caffeine complex. Caffeine is also able to block potential DNA binding site or remove the antibiotic already complexed with DNA, particularly in case of daunomycin. The relative importance of each process, hetero-association or competition for binding site on DNA, depends upon several factors. The specific conjugated aromatic ring

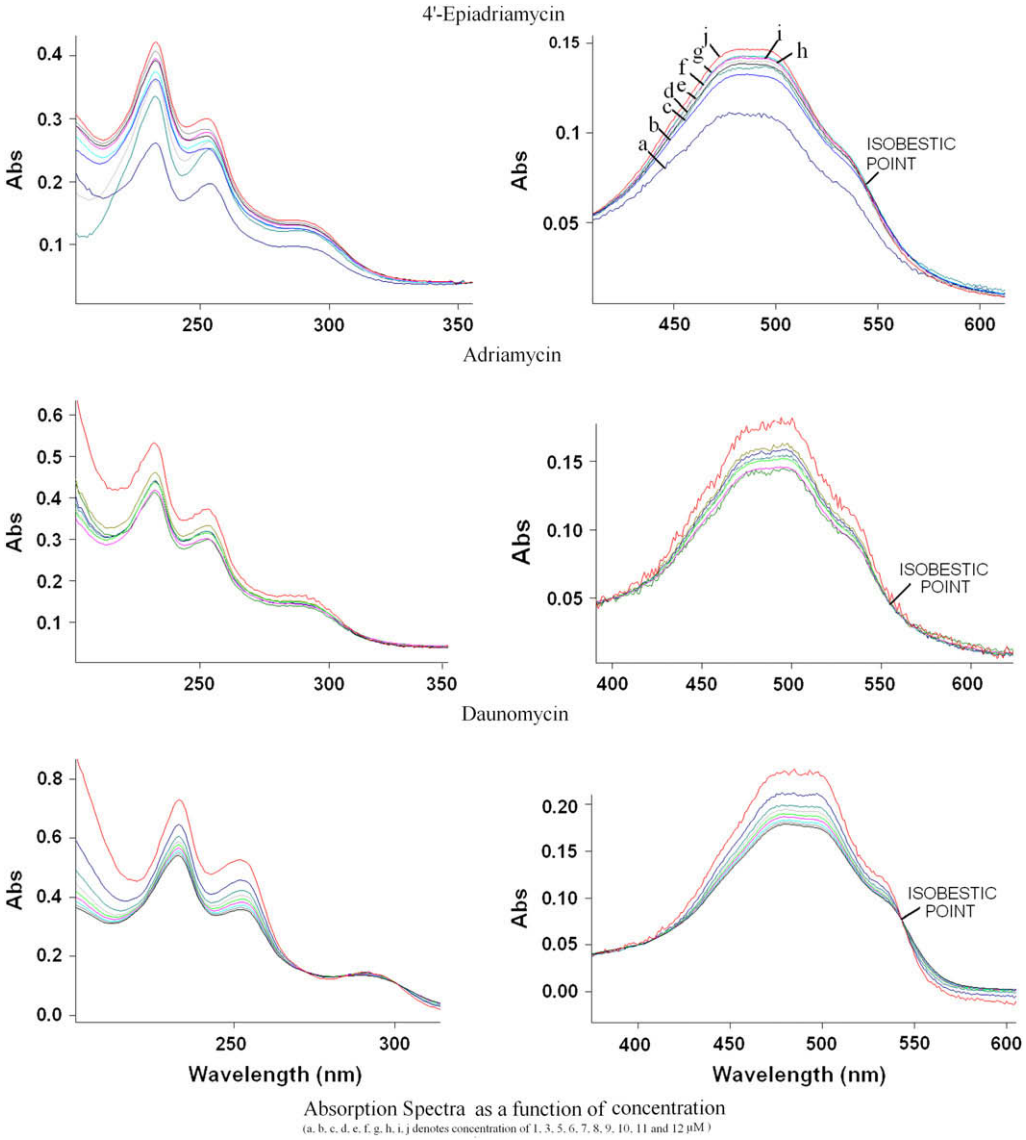

Fig. 8. Absorption spectra of 4′-epiadriamycin, adriamycin and daunomycin as a function of concentration (a, b, c, d, e, f, g, h, i, j denote concentration of 1, 3, 5, 6, 7, 8, 9, 10, 11 and 12 μM, respectively).

system of anthracycline/anthraquinone and the side chains will influence van der Waals dispersive forces responsible for overlap of aromatic rings, inter-molecular interactions with side chains attached to aromatic ring, steric factors, hydrophobicity and inter-molecular hydrogen bonding. It has been suggested [32] that the scavenging effect of cell detoxification can be used as a potential strategy of regulation of medico-biological activity of these drugs in clinical practice, say for example in reduction of the consequences of drug's overdosing during chemotherapy or in production of anti-mutagenic effects in vivo.

Our results from physico-chemical techniques and restrained molecular dynamics indicate that there are specific differences in stacked structure of the three drugs. The stacked structure of 4′-epiadriamycin is better stabilized by dispersive forces due to reduced angles between planes of aromatic rings (13° for parallel orientation) resulting in immobilization of hydroxyl and NH_3^+ moieties, higher K_{eq} value and decreased diffusion constant in DOSY spectra. It has been shown that conformer (2) corresponding to glycosidic angle C7–O7–C1′–C2′ = 127–144° is the biologically relevant conformer [33–35]. The readiness, with which 4′-epiadriamycin adopts this conformation in both parallel and anti-parallel orientation, shows that its anti-proliferative activity is certainly not compromised as compared to daunomycin and adriamycin in spite of better self-association. A relatively more stable dimer of 4′-epiadriamycin may initially slow down uptake of drug through the cell membrane. However, once absorbed, it may not let the drug get ejected out through channel across membrane, increasing thereby the efficacy of the drug.

2.6.2. Toxicity

The ability to generate oxygen radicals during redox cycling and in vitro reductive glycosidic cleavage through the formation of tautomer 7-deoxydaunomycinone [36,37] is known to be responsible for cardiotoxicity. The kinetics of sugar moiety detachment has been related to conformation of cyclohexyl ring A [38]. Our results from mass spectra have given a direct proof of cleavage and clearly show that it is negligible in 4′-epiadriamycin. These results may well explain why 4′-epiadriamycin developed recently is better tolerated due to lesser cardiotoxicity than adriamycin and daunomycin [3].

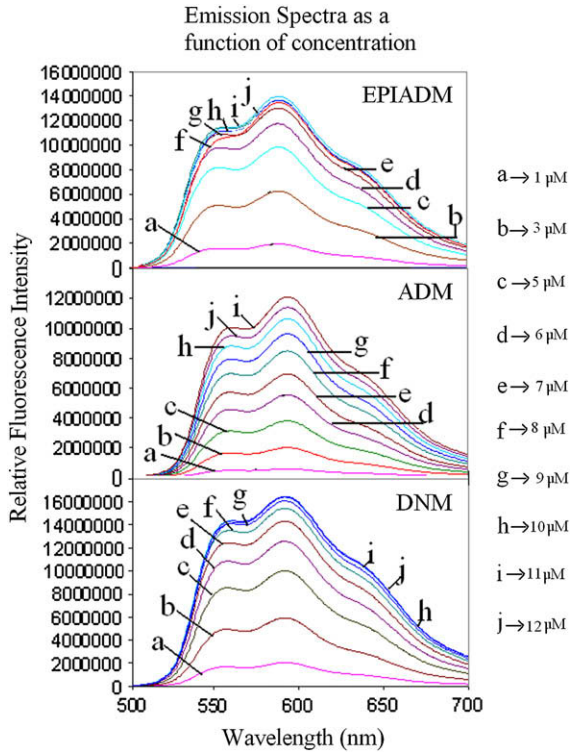

Fig. 9. Emission spectra of 4′-epiadriamycin (EPIADM), adriamycin (ADM) and daunomycin (DNM) as a function of concentration (a, b, c, d, e, f, g, h, i, j denote concentration of 1, 3, 5, 6, 7, 8, 9, 10, 11 and 12 μM, respectively).

3. Summary and conclusions

1D proton NMR of various drugs shows upfield shifts upto 0.68 ppm in ring A and ring D on increasing concentration from 0.01 to 8.00 mM. This is attributed to the stacking of the chromophore rings. Temperature dependence studies show downfield shift upto 0.81 ppm with temperature for the aromatic protons indicating that these drugs exist in aggregated form. 2D NOESY spectra at 355 K show various inter-molecular and intra-molecular cross-peaks, which are evolved due to the stacking of aromatic chromophores of drug molecules. Restrained molecular dynamics studies show the existence of parallel and anti-parallel orientations between two aromatic rings in the dimer. To date no such structure of dimer has been reported for the 4′-epiadriamycin and adriamycin. The results in literature for daunomycin [15] have structure similar to that observed by us although we get more inter-molecular contacts. Absorption and fluorescence studies show that aggregation starts at low concentration ~10 μM and the observed isobestic point for absorption spectra is 545 nm. The DOSY studies indicate that the rate of diffusion increases in the following manner 4′-epiadriamycin < adriamycin < daunomycin. ESI-MS experiments clearly demonstrate the existence of dimers. Higher aggregates are not observed. The mass spectra of adriamycin and daunomycin also show presence of 7-deoxydaunomycinone resulting from cleavage of glycosidic bond. Absence of cleaved moiety in 4′-epiadriamycin gives the direct proof of reduced cardiotoxicity due to generation of free radicals following the cleavage of glycosidic bond. The structural difference between stacked dimer of the three drugs may be related to competitive binding with DNA and hence different in their pharmacological action.

4. Materials and methods

4′-Epiadriamycin was purchased from Calbiochem Pvt. Ltd., San Diego, CA, USA. Adriamycin, daunomycin and deuterium oxide were purchased from Sigma–Aldrich Chemicals Ltd., St. Louis, MO, USA. All other chemicals, like Na_2HPO_4 and NaH_2PO_4, sodium 2,2-dimethyl-2-silapentane-5-sulphonate (DSS), an internal NMR reference, were purchased from Merck Sharp and Dohme Ltd., Quebec, Canada. Typically 1 μl of 0.1 M solution of DSS was added to all the three drugs as an internal reference.

4.1. NMR studies

Experiments were carried out on Bruker Avance 500 MHz spectrophotometer. Typical parameters for 1D NMR experiments were: number of data points 32–64 K, spectral width 5000 Hz, number of scans 64–128 and digital resolution 0.30 Hz/point and relaxation delay 2.0 s. Receiver gain was optimized to obtain the best possible signal to noise ratio. 1D NMR was recorded as a function of temperature as well as concentration. The solvent suppression was done by using the standard pre-saturation method in which the water signal was pre-saturated by applying a low power continuous wave irradiation on its signal during the pre-scan period. The power level and duration of pre-saturation were 58.86 dB and 2.0 s, respectively. The concentration dependence of the proton chemical shifts of drug molecules were determined at 298 K over the concentration range of 0.01–8.00 mM; the temperature dependences of the proton chemical shifts were measured over the temperature range 275–355 K at a concentration of 8 mM for all the three drugs. 2D NOESY experiments were carried out at 355 K in D_2O. Typical parameters for 2D experiments were 1024–2048 data points along t2 dimension, 512 free induction decays in t1 dimension, pulse width ~7.7 μs, spectral width 6000 Hz (^{1}H), number of scans 64, digital resolution 3.0 Hz/point and relaxation delay 2.0 s, mixing time 400 ms. The processing was done by Topspin 1.3 version software. Data was zero filled in F1 dimension before Fourier transformation. Sine squared bell window function was applied before processing the FIDs. The inter-proton distances were calculated from the NOESY spectra recorded at $\tau_m = 400$ ms by integrating the volume of each cross-peak. The integration method was based on isolated spin pair approximation in which spin diffusion effect was not taken into account, as the affect was negligible, therefore not considered during inter-proton distance calculations. The distance between 1H and 2H protons, r (1H–2H) = 2.50 Å, was used as an internal reference [24]. Pseudo-atom corrections were used for methyl and other equivalent protons.

4.2. Restrained molecular dynamics simulations

The initial structure of the dimer models of 4′-epiadriamycin, adriamycin and daunomycin had been built using builder module in INSIGHT II, version 2005 (Accelrys Inc., San Diego, California) software. The energy of the molecule was minimized using 1000 steps each of Steepest Descent and Conjugate Gradient to remove any internal strain due to short contacts in starting structure using CFF91 force field [39,40] in DISCOVER software version 2005 (Accelrys Inc., San Diego, California). Dielectric constant was fixed as 1.0 for calculation of electrostatic interactions. Conformational search was performed by using the following simulated annealing restrained Molecular Dynamics protocol. The molecule was heated to a temperature of 800 K in steps of 100 K so that the chances of molecule being trapped in local minima become least and it can reach global minima. Molecular Dynamics was carried out for 100 ps (1000 iterations with time step of 1 fs) at 800 K during which 100 structures were saved at regular intervals of 1 ps. Each of them was then slowly cooled at 300 K in steps of 100 K. The NOEs were categorized as strong, medium, and weak with the corresponding distances set in the range 1.8–2.4 Å, 2.5–2.9 Å, and 3.0–4.5 Å respectively. The force constants for NOEs for the corresponding peaks were held constant as 25, 15 and 10 kcal mol^{-1} Å^{-2},

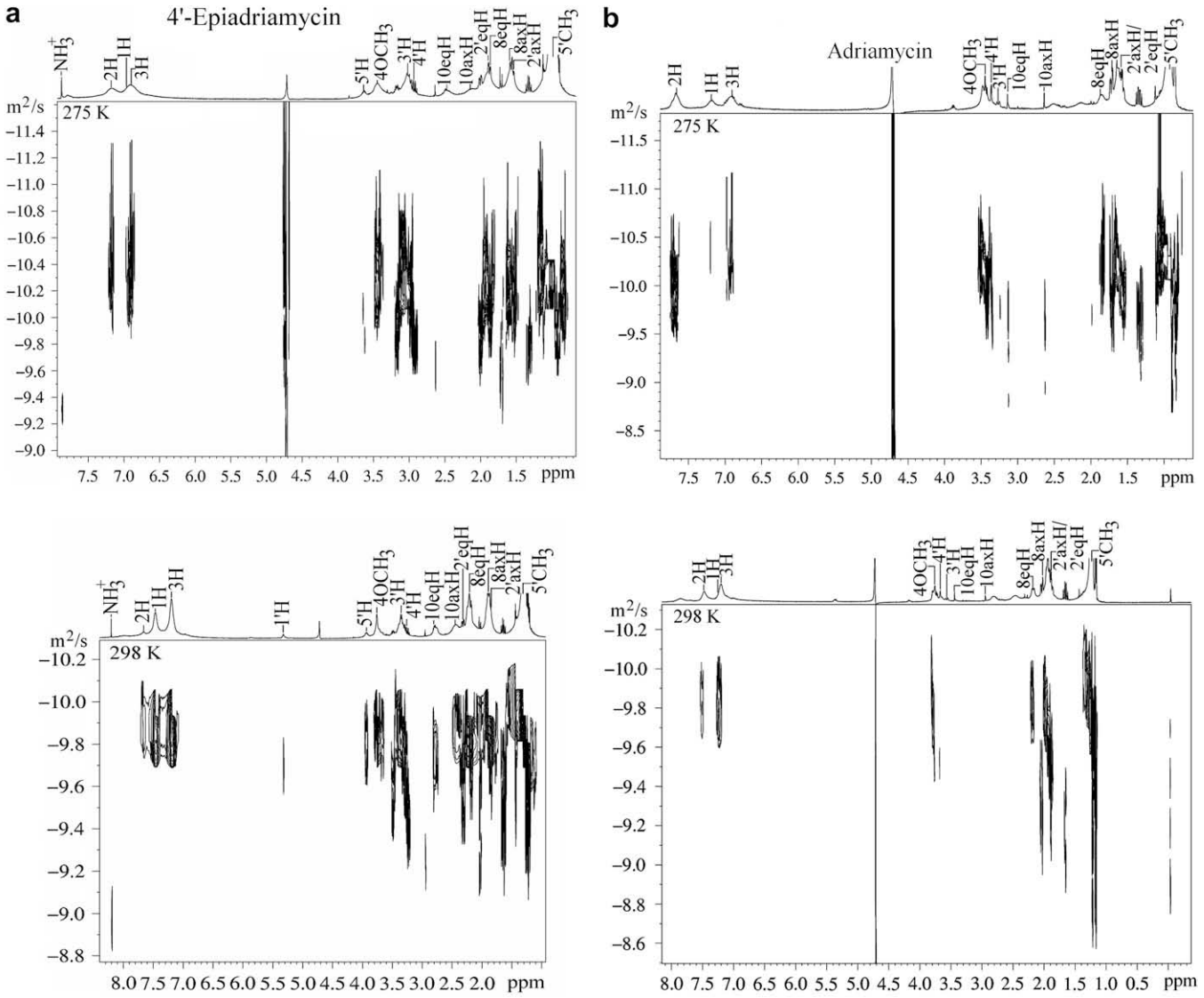

Fig. 10. (a–c) DOSY spectra of 8 mM concentration of (a) 4′-epiadriamycin, (b) adriamycin and (c) daunomycin in D_2O at 275 and 298 K.

respectively. At the end of simulated annealing, all the structures were minimized by 1000 steps of Conjugate Gradient until a predefined convergence limit of root mean square derivative of <0.001 kcal mol^{-1} Å^{-1} was reached. Same protocol was repeated for the other two drugs, adriamycin and daunomycin to see the difference due to their slight variation in structures.

4.3. UV–vis and fluorescence spectroscopic studies

UV–vis absorbance spectra were recorded in CARY 100 Bio spectrophotometer. Emission scan was done in Spectrofluorimeter (model Fluorolog-3, make HORIBA Jobin Yvon Spex). The concentration of 4′-epiadriamycin, adriamycin and daunomycin in buffer solution were determined spectrophotometrically at the λ_{max} of 480 nm ($\varepsilon = 11{,}500$ M^{-1} cm^{-1}). All experiments were performed in the standard buffer containing 70 mM NaCl, 20 mM phosphate buffer, pH = 7.0 at 25 °C. The buffer was filtered through 0.45 μm pore Millex Millipore filters. Absorbance and emission scans were done from 1, 3, 5, 6, 7, 8, 9, 10, 11, 12 μM concentration. The absorbance as well as relative fluorescence versus concentration study was made to find the presence of self-association of the drugs. Dimerization constant was calculated using least square-fitting curve [41–43]. The ligand dimerization constants (K_D) were calculated according to the method described by von Tscharner and Schwarz [44]:

$$K_D = C_T - C_M/2C_M^2$$

where C_T was the total ligand concentration and C_M was the monomer concentration. The wavelength for maximum absorbance was 480 nm and the isobestic point was at 545 nm. The absorption spectrum of adriamycin, 4′-epiadriamycin and daunomycin had three bands in the visible region (529, 496, 479 nm) and three in the UV region (288, 252, 233 nm) [27]. In the fluorescence spectrum, excitation wavelength (λ_{ex}) of 480 nm and emission wavelength (λ_{em}) of 592 nm was used.

4.4. Diffusion Ordered Spectroscopy (DOSY)

The DOSY experiment was the measure of diffusion coefficients by NMR. In DOSY spectra, chemical shift was detected along the *F*2 axis and diffusion coefficient was along the *F*1 axis. We had used the method developed by Stejskal and Tanner (1965), which relies

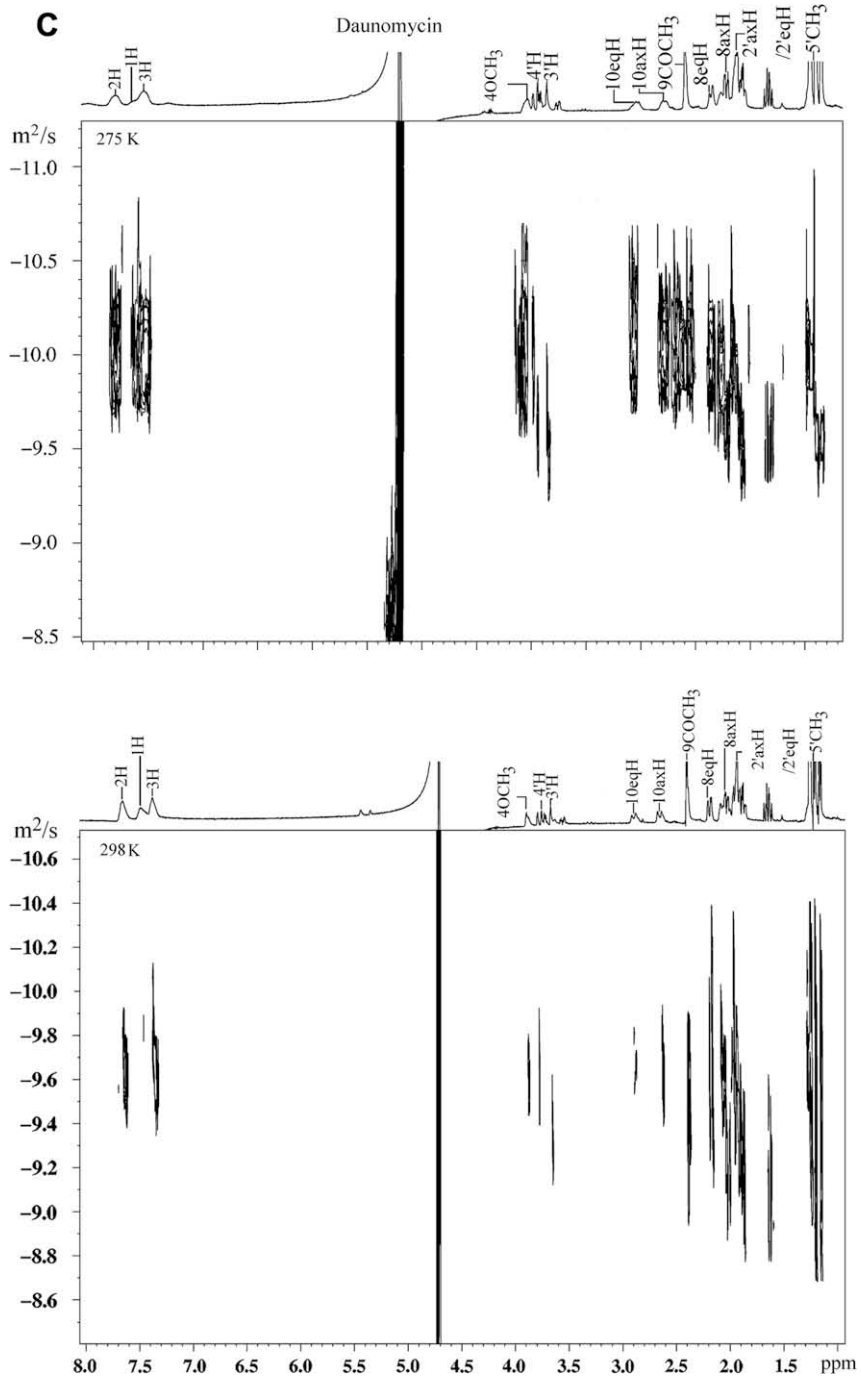

Fig. 10. (*continued*).

on two gradient pulses surrounding the 180° pulse in the spin echo. The first gradient dephases the transverse magnetization in a spatially dependent manner along the *z*-axis and the second gradient then rephases the magnetization. The relation between translational self-diffusion and the measurable NMR parameters (Stejskal and Tanner, 1965) was:

$$A/A_0 = -\exp\left[D_t\gamma_H^2\delta^2G_z^2(\Delta - \delta/3)\right]$$

where A was the measured peak intensity (or volume), A_0 was the maximum peak intensity, D_t was the translational diffusion constant (in cm^2/s), γ_H was the gyromagnetic ratio of a proton ($2.675197 \times 10^4\ G^{-1}\ s^{-1}$), δ was the duration of the gradient, Δ was the time between gradients and G_z was the strength of the gradient (in G/cm). Data can be plotted as $-\ln(A/A_0)$ versus $\gamma_H^2\delta^2G_z^2(\Delta - \delta/3)$. The slope of the line gives the value of D_t. The pulse program used was pulsed gradient spin echo (stimulated echo sequence incorporating bipolar gradients) sequence modified with binomial water suppression. The gradient strengths were incremented as a square dependence in the range from 1 to 32 G cm^{-1}. The diffusion time (Δ) and the duration of the magnetic field gradients (δ) were 100 and 6 ms, respectively. Other parameters include a sweep width of 6000 Hz, 32 K data points, 1024 transients and an acquisition time of 2.7 s and relaxation delay of 2.0 s.

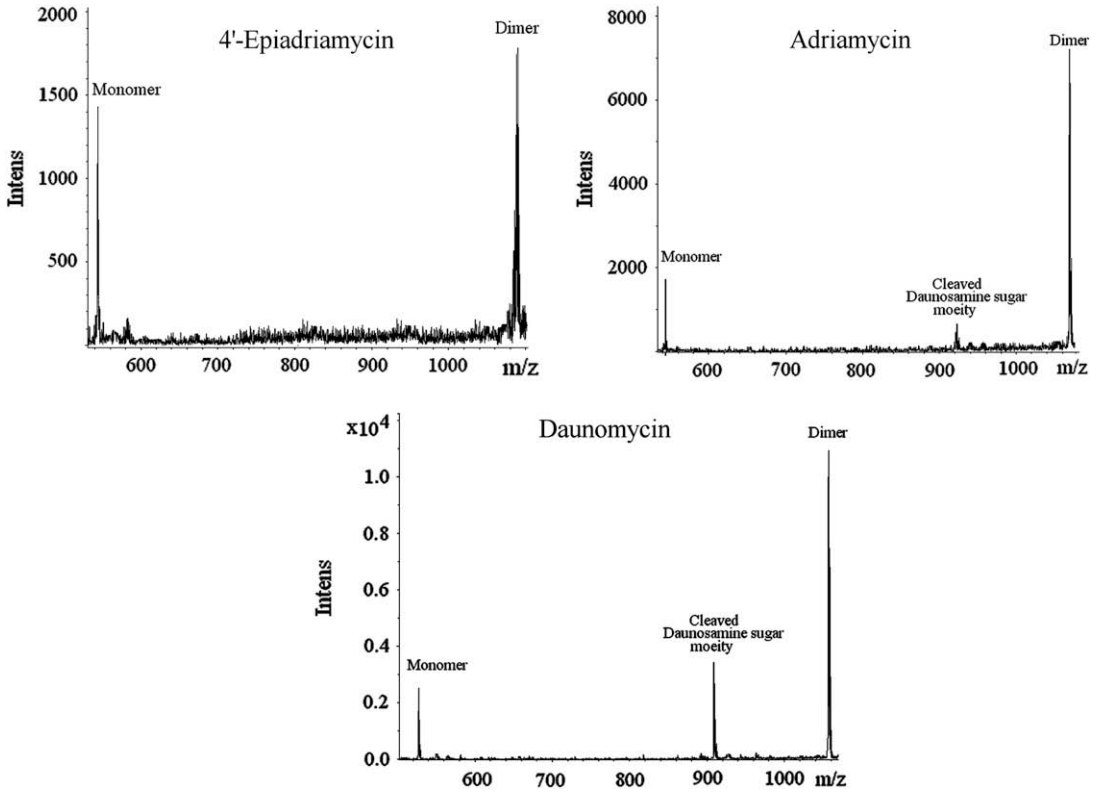

Fig. 11. Electron Spray Ionization Mass Spectra (ESI-MS) of the 5 μM concentration anthracycline drugs showing that the drugs exist in monomeric and dimeric states with single charge.

However, it was critical to calibrate the gradient coils before the acquisition of the data. For the calibration [45] of the gradient hardware and probe, a sample of 100% D_2O in an NMR tube was used. The calibrations involved measurement of the maximum strength of the gradient pulse, characterization of the eddy-current recovery time for the probe, and examination of the linear power response of the *z*-axis gradients. The method depends on the acquisition of a spin-echo FID of the calibration sample with the *z*-axis gradient on during acquisition, which yielded a spatial profile of the sample, which was the function of the sample height and the gradient strength, Gz. The eddy-current recovery time was examined using a pulse sequence in which a full-strength gradient pulse was applied for 10 ms (a longer time than was used in the experiments) followed by an adjustable time delay and then a 90° proton observation pulse. Data were collected on the residual proton water signal in the calibration sample. It was found that there was complete eddy-current relaxation within less than 1 ms for the triple-resonance probe used in these experiments. Hence we needed to wait longer than 1 ms after applying the gradients in the stimulated echo sequence. It was assured that the *z*-axis gradients be linear in the volume occupied by the sample, and respond linearly to the power applied. So the measurements were made using the pulsed gradient spin echo (stimulated echo sequence incorporating bipolar gradients) sequence of the residual proton signal in the calibration sample over a large range of δ and Δ times. The data gave the same D_t value for each value of δ and Δ, and the plot of $-\ln(A/A_0)$ versus $\gamma_H^2\delta^2G_z^2(\Delta - \delta/3)$ was a straight line, which demonstrated the linear gradient power response required.

4.5. Electron Spray Ionization Mass Spectrometry studies (ESI-MS)

Positive-ion ESI-MS spectra were obtained on Esquire 4000 (Bruker Daltonics, Germany) with the normal ESI source. The 5 μM concentration solutions of the drugs were prepared in the water:acetic acid mixture in the ratio of 90:10. The solutions were infused directly into the mass spectrometer at 240 μl/h rate. The parameters selected were: cone voltage 4.0 kV, nebulizer pressure 15 psi, dry gas flow rate 8 l/min and the capillary temperature 100 °C. Data was collected for approximately 10 scans. The maximum accumulation time was 200 ms and scan range was 400–1700 *m*/*z*.

Acknowledgements

The use of Bruker Avance 500 MHz FT NMR at Central NMR Facility, Indian Institute of Technology Roorkee (IITR), Roorkee is gratefully acknowledged. Council of Scientific and Industrial Research (CSIR), Govt. of India, is gratefully acknowledged for a senior research fellowship provided to Ms. Prashansa Agrawal.

Appendix. Supplementary data

Supplementary data associated with this article can be found in the online version, at doi:10.1016/j.ejmech.2008.09.037.

References

[1] F. Arcamone, S.T. Crooke, S.D. Reicin (Eds.), Doxorubicin: Anticancer Antibiotics, Medicinal Chemistry, vol. 17, Academic Press, New York, 1981, pp. 1–369.
[2] S. Neidle, M.R. Sanderson, S. Neidle, M.J. Waring (Eds.), Molecular Aspects of Anticancer Drug Action, vol. 35, Macmillan, London, 1983, pp. 35–57.
[3] F. Arcamone, S. Penco, J.W. Lown (Eds.), Anthracycline and Anthracenedione Base Anticancer Agents, Elsevier, New York, 1988.
[4] J.B. Chaires, N. Dattagupta, D.M. Crothers, Biochemistry 21 (1982) 3927–3932.
[5] V. Barthalemy-Clavey, J.C. Maurizot, J.L. Dimicoli, P. Sicand, FEBS Lett. 46 (1974) 5–10.
[6] S. Eksborg, J. Pharm. Sci. 67 (1978) 782–785.
[7] H. Schutz, F.A. Gollmick, E. Stutter, Stud. Biophys. 75 (1979) 147–159.
[8] S.R. Martin, Bioploymers 19 (1980) 713–721.
[9] R.B. Martin, Chem. Rev. 96 (1996) 3043–3064.
[10] J.W. Lown, C.C. Hanstock, J. Biomol. Struct. Dyn. 2 (1985) 1097–1106.

[11] J. Kotovych, J.W. Lown, P.K. Tong, J. Biomol. Struct. Dyn. 4 (1986) 111–125.
[12] D.B. Davies, D.A. Veselkov, L.N. Djimant, A.N. Veselkov, Eur. Biophys. J. 30 (2001) 354–366.
[13] N. Veselkov, M.P. Evstigneev, S.A. Vysotskii, D.A. Veseklov, D.B. Davies, Biophysics 47 (2002) 432–438.
[14] D.B. Davies, D.A. Veselkov, M.P. Evstigneev, A.N. Veselkov, J. Chem. Soc., Perkin Trans. 2 (2001) 61–67.
[15] M.P. Evstigneev, V.V. Khomich, D.B. Davies, Russ. J. Phys. Chem. 80 (2006) 741–746.
[16] C.S. Johnson, Prog. Nucl. Magn. Reson. Spectrosc. 34 (1999) 203–256.
[17] M.D. Diaz, S. Berger, Carbohyd. Res. 329 (2000) 1–5.
[18] W. Bocian, R. Kawecki, E. Bednarek, J. Sitkowski, New J. Chem. 30 (2006) 467–472.
[19] N.E. Schlorer, E.J. Cabrita, S. Berger, Angew. Chem., Int. Ed. 41 (2002) 107–109.
[20] E.J. Cabrita, S. Berger, P. Brauer, J. Karger, J. Magn. Reson. 157 (2002) 124–131.
[21] F. Rosu, S. Pirotte, E.D. Pauw, V. Gabelica, Int. J. Mass Spectrom. 253 (2006) 156–171.
[22] A. Triolo, F.M. Arcamone, A. Raffaelli, P. Salvadori, J. Mass Spectrom. 32 (1997) 1186–1194.
[23] K.X. Wan, T. Shibue, M.L. Gross, J. Am. Chem. Soc. 122 (2000) 300–307.
[24] R. Barthwal, N. Srivastava, U. Sharma, G. Govil, J. Mol. Struct. 327 (1994) 201–220.
[25] R. Barthwal, A. Mujeeb, N. Srivastava, U. Sharma, Chemico-Biol. Interact. 100 (1996) 125–139.
[26] M. Trieb, C. Rauch, B. Wellenzohn, F. Wibowo, T. Loerting, E. Mayer, K.R. Liedl, J. Biomol. Struct. Dyn. 21 (2004) 713–723.
[27] A. Di Marco, M. Gaetani, B. Scarpinato, Cancer Chemother. R4 53 (1969) 33–37.
[28] D.S. Alberts, S.E. Salmon, E.A. Surit, H.S.G. Chen, T.E. Moon, F.L. Meyskens, Proc. Am. Assoc. Cancer Res. 23 (1981) 153–175.
[29] A.L. Adel, R.T. Dorr, J.D. Liddil, Cancer Invest. 11 (1993) 15–24.
[30] J. Piosik, M. Zdunek, J. Kapuscinski, Biochem. Pharm. 63 (2002) 635–646.
[31] F. Traganos, J. Kapuscinski, Z. Darzynkiewicz, Cancer Res. 51 (1991) 3682–3689.
[32] M.P. Evstigneev, V.V. Khomich, D.B. Davies, Eur. Biophys. J. 36 (2006) 1–11.
[33] M.H. Moore, W.H. Hunter, L. d'Estaintot, O. Kennard, J. Mol. Biol. 206 (1989) 693–705.
[34] C.M. Nunn, L.W. Meervelt, S. Zhang, M.H. Moore, O. Kennard, J. Mol. Biol. 222 (1991) 167–177.
[35] A.H.J. Wang, G. Ughetto, G.J. Quigley, A. Rich, Biochemistry 26 (1987) 1152–1163.
[36] S. Pan, N.R. Bachur, Mol. Pharmacol. 17 (1980) 95–98.
[37] D.L. Kleyer, T.H. Koch, J. Am. Chem. Soc. 105 (1983) 2504–2509.
[38] V. Malatesta, S. Penco, N. Sacchi, L. Valentini, A. Vigevani, F. Arcamone, Can. J. Chem. 62 (1984) 2845–2853.
[39] J.R. Maple, T.S. Thacher, T. Dunir, A.T. Hagler, Chem. Des. Automation News 5 (1990) 5–10.
[40] J.R. Maple, T. Dunir, A.T. Hagler, Proc. Natl. Acad. Sci. U.S.A. 85 (1988) 5350–5354.
[41] J. Kapuscinski, Z. Darzynkiewicz, Biochem. Pharmacol. 34 (1985) 4203–4213.
[42] B.S. Lee, P.K. Dutta, J. Phys. Chem. 93 (1989) 5665–5672.
[43] D.H. Bell, Biochim. Biophys. Acta 949 (1989) 132–137.
[44] V. Von Tscharner, G. Schwarz, Biophys. Struct. Mech. 5 (1979) 75–78.
[45] J. Lapham, J.P. Rife, P.B. Moore, D.M. Crothers, J. Biomol. NMR 10 (1997) 255–262.